

Electrical Characteristics of Quaternary Layered Structured $\text{Tl}_4\text{In}_3\text{GaS}_8$ Crystals

Jazi Abdullah Mohammed Abdulwahed

Physics Department, Umm Al-Qura University College, Qunfudah, KSA

Email address:

jaabdulwahed@uqu.edu.sa

To cite this article:

Jazi Abdullah Mohammed Abdulwahed. Electrical Characteristics of Quaternary Layered Structured $\text{Tl}_4\text{In}_3\text{GaS}_8$ Crystals. *American Journal of Science, Engineering and Technology*. Vol. 8, No. 4, 2023, pp. 206-209. doi: 10.11648/j.ajset.20230804.15

Received: October 2, 2023; Accepted: October 26, 2023; Published: November 9, 2023

Abstract: Despite the fact that numerous compositions of quaternary chalcogenides have recently been identified as having high thermoelectric capabilities and are still being studied for energy applications, experimental data on the electrical characteristics of $\text{Tl}_4\text{In}_3\text{GaS}_8$ crystals is scarce. In this paper, growing quaternary $\text{Tl}_4\text{In}_3\text{GaS}_8$ layered crystals have been prepared using the travelling solvent method (TSM). In this investigation, we evaluated the electrical conductivity and Hall effect measurements in the temperature range of 203 K to 443 K. These measurements allowed the determination of many physical parameters for both the majority and minority carriers, including carrier mobility, resistivity, carrier concentration, Hall coefficient, and conductivity. Our research revealed that our samples are n-type conductors. From the electrical conductivity and Hall effect studies, the forbidden energy gap and the impurity level's ionisation energy were determined for the crystals studied. At room temperature, the electrical conductivity, Hall coefficient, and carrier concentration were $0.85 \Omega^{-1}\text{cm}^{-1}$, $21.8 \text{ cm}^3\text{C}^{-1}$, and $2.997 \times 10^{29} \text{ cm}^{-3}$, respectively. Also, the Hall mobility was found to be $0.177 \text{ cm}^2/\text{V} \cdot \text{sec}$.

Keywords: Crystal Growth, $\text{Tl}_4\text{In}_3\text{GaS}_8$, DC Electrical Conductivity, Hall Coefficient, Characterization of Semiconducting Quaternary Compounds

1. Introduction

Quaternary chalcogenides are a broad family of materials that are primarily composed of earth-abundant elements and are of interest for solar-cell absorber applications [1], photocatalysts for solar water decomposition [2], magneto-optical and magnetic iron materials [3, 4]. Using the varied heating rates approach, trapping centers with activation energies of 12 meV were found in as-grown $\text{Tl}_4\text{In}_3\text{GaS}_8$ crystals. The activation energy was measured and compared to that found in photoluminescence tests [5].

This work extends the research on quaternary chalcogenides with new compositions and structural types and advances basic research on multinary chalcogenides for electrical applications. The layered semiconductor group includes the quaternary $\text{Tl}_4\text{In}_3\text{GaS}_8$ crystal. This chemical is a structural analog of TlInS_2 , with gallium ions replacing a fourth of the indium ions [6]. There is currently very little information available on the physical properties of this compound. In recent years, no research on the electrical conductivity and Hall effect of $\text{Tl}_4\text{In}_3\text{GaS}_8$ crystals has been

published. The main goals of this study were to prepare $\text{Tl}_4\text{In}_3\text{GaS}_8$ and to establish for the first time the temperature dependence of electrical conductivity and Hall coefficient.

2. Experimental

In our crystal-growth laboratory, the modified Bridgman method was used to prepare $\text{Tl}_4\text{In}_3\text{GaS}_8$ crystals from a stoichiometric melt of starting materials sealed in an evacuated (10^{-6} Torr) silica tube (10 cm long and 1.5 cm in diameter) with a tip at the bottom. The processes of growth as well as the experimental apparatus have been detailed elsewhere [7]. By this procedure, calculated amounts of the pure Tl, In, Ga, and S (6N) elements (Aldrich Mark) were mixed according to my calculations, to prepare 15 gm of $\text{Tl}_4\text{In}_3\text{GaS}_8$: Tl (3.80 gm), In (2.80 gm), Ga (1.2 gm), and S (7.2 gm). The resulting ingot is yellow-green in colour, with mirror-like freshly cleaved surfaces. Silver paste was used to make electrical contacts on the sample's opposite sides, and the contacts' ohmic nature was confirmed accordingly. For circuit connection, thin copper wires were added to the

electrodes. The examined sample had n-type electrical conductivity. For all measurements, a vacuum cryostat with a local design and a Tensely UJ33E potentiometer with a field strength of 0.5 tesla were used. The electrical measurements were carried out with liquid nitrogen to generate dense data over the 203–443 K temperature range. In a unique cryostat using a traditional DC-type measuring system, the conductivity and Hall coefficient were measured using a compensation technique. To avoid the Hall voltage, drop when the length-to-width ratio of the sample is smaller than three, as discussed by Isenberg [8], the samples with diameters of $10.4 \times 3.5 \times 2.7 \text{ mm}^3$ were chosen for electrical conductivity and Hall effect studies. The Hall contacts were virtually infinitely tiny; so, the current flow was not distorted. The temperature of every specimen was measured with the help of a copper-constantan thermocouple. When the current was orientated at right angles to the c-axis, the electrical conductivity σ_{\perp} was measured.

3. Results

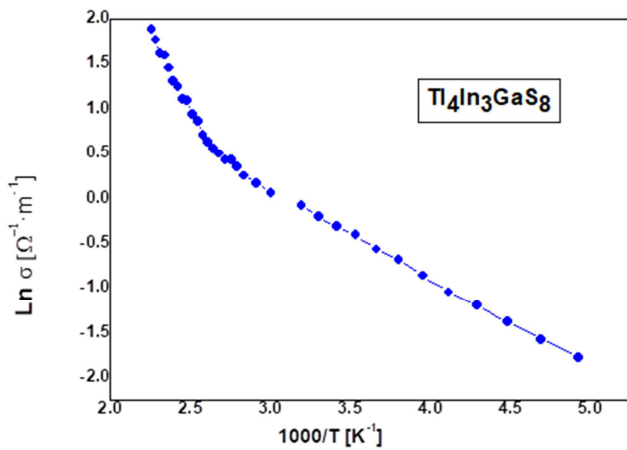


Figure 1. Arrhenius plots of electrical conductivities for $\text{Ti}_4\text{In}_3\text{GaS}_8$ crystals.

The variation in direct current conductivity with inverse temperature from 203 to 443 K is depicted in Figure 1.

As the temperature rises, the conductivity of the $\text{Ti}_4\text{In}_3\text{GaS}_8$ samples rises as well, showing semiconducting behaviour. Because the main role is played by free carrier transition from the impurity level at low temperatures (the extrinsic zone), the carrier concentration can be dictated by the quantity of ionised donors. As a result, the conductivity grows slowly.

The ionisation energy of impurities, ΔE_d , was computed and determined to be 0.17 eV. The conductivity rises rapidly at high temperatures (390 - 443 K) due to a rapid increase in total carrier density. This suggests that at high temperatures, the intrinsic conductivity becomes more favourable. The width of the energy gap was calculated to be 0.61 eV. Between 309 and 334 K, the intermediate area can also be seen. The temperature at which from transitions impurity to intrinsic conductivity is determined by the impurity concentration in the semiconductor. The rise in electrical conductivity in this middle zone is attributable to an increase

in mobility since the carrier density in this temperature region remains almost constant until the intrinsic region is reached. The temperature dependences show a change from a lower slope to a higher slope zone. At room temperature, $\text{Ti}_4\text{In}_3\text{GaS}_8$ samples have a conductivity of $0.85 \Omega^{-1}\text{cm}^{-1}$.

Figure 2 shows the relationship between the Hall coefficients and the temperature of the sample examined. The sample examined was found to be n-type. At room temperature, the Hall coefficient has a value of $21.8 \text{ cm}^3\text{C}^{-1}$. This figure shows the general behaviour of the Hall coefficient with temperature. From the curve in Figure 2, the three regions can clearly be distinguished. In the intrinsic region, the Hall coefficient varies linearly and rapidly with temperature, whereas it varies slowly with temperature in the impurity region. An intermediate region has been discovered between these two regions. Figure 3 represents the relation between $R_H T^{3/2}$ and $10^3/T$. It's usually separated into two parts: the first at low temperatures, where $R_H T^{3/2}$ slowly reduces as the temperature rises. This region indicates the extrinsic part from which the position of the donor level is calculated as $\Delta E_d = 0.13 \text{ eV}$, and the second at higher temperatures. The second part is over 430 K. This is the region in which the $R_H T^{3/2}$ decreases rapidly with increasing temperature and is known as the intrinsic region. The forbidden bandwidth is calculated from these figures and has a value of 0.36 eV. Charge carrier mobility can be determined by simultaneously measuring conductivity and Hall constants.

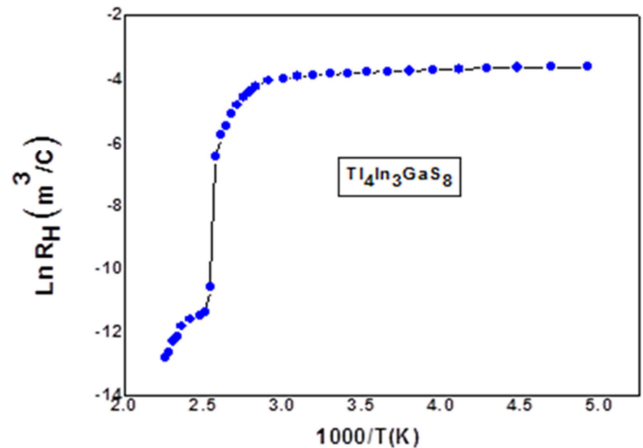


Figure 2. Dependence of the Hall effect on the reciprocal of the temperature for $\text{Ti}_4\text{In}_3\text{GaS}_8$ crystals.

Two factors determine the temperature dependency of the Hall mobility of current carriers: phonon scattering and ionised impurity scattering. Figure 4 shows the temperature reliance of the Hall mobility of current carriers in $\text{Ti}_4\text{In}_3\text{GaS}_8$ crystals, $\mu = R_H \sigma$. Two distinct temperature areas may be seen, each with a different slope. In the first region at low temperature, according to $\mu \propto T^3$, mobility appears to increase with temperature. This behavior agrees with the Hall mobility of semiconductor behavior. Because the exponent value and sign suggest such a component of scattering, such behaviour is typical of charge carrier

scattering with ionised impurities. In the high temperature region, the Hall mobility decreases with increasing temperature. During this region, μ_H decreases with increasing temperature and obeys the law $\mu_H T^{-3/2}$. In comparison to the real values, it appears that the value of the exponent n inside the relation $\mu_H T^n$ is typically large compared with scattering in other semiconductors. But such behavior was observed earlier throughout the investigation of TiGaSeS [9], $\text{Ti}_2\text{GaInTe}_4$ [10], CuInGaSe_2 [11], and $\text{Cu}_2\text{ZnGeS}_4$ [12]. This behavior in our opinion, could also be related to the presence of a high density of stoichiometric vacancies and, therefore, the creation of defects. At room temperature, the mobility of charge carriers can be decided as $0.177 \text{ cm}^2/\text{V}\cdot\text{sec}$. $\text{Ti}_4\text{In}_3\text{GaS}_8$ has much higher charge carrier mobility than comparable AIII BVI group semiconducting materials [13]. Hall estimations are an exceptionally valuable procedure in examining the temperature effect on the carrier concentrations. Figure 6 shows how the concentration of electron carriers increases rapidly with temperature in the high temperature zone but slowly in the low temperature zone.

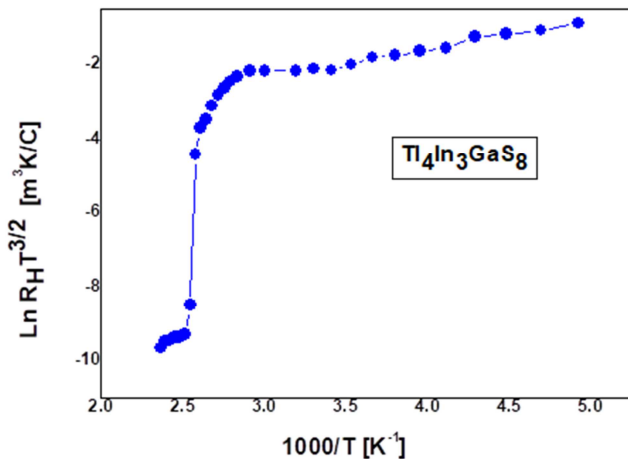


Figure 3. Arrhenius plots of Hall effect for $\text{Ti}_4\text{In}_3\text{GaS}_8$ crystals.

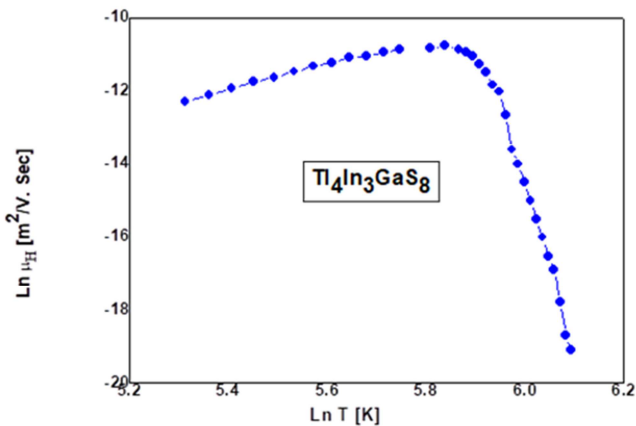


Figure 4. Mobility vs. the temperature for $\text{Ti}_4\text{In}_3\text{GaS}_8$ crystals.

According to the Hall coefficient, the carrier concentrations at 300 K are $2.9 \times 10^{23} \text{ m}^{-3}$. At room temperature, the relaxation time and diffusion length of

electrons are calculated to be $1.8 \times 10^{-19} \text{ sec}$ and $6.6 \times 10^{-23} \text{ cm}$, respectively.

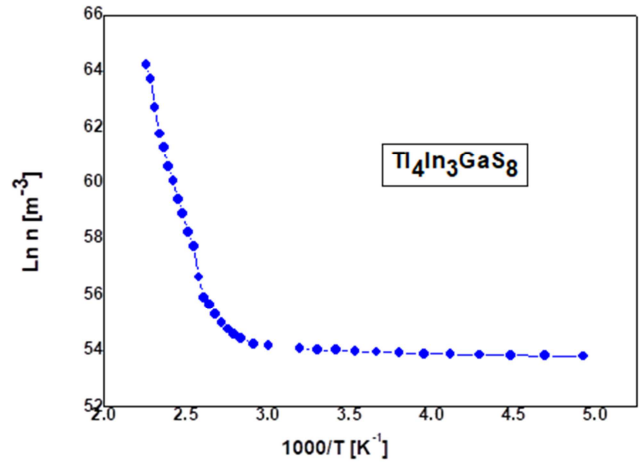


Figure 5. Hole concentration vs. reciprocal temperature for $\text{Ti}_4\text{In}_3\text{GaS}_8$ crystals.

4. Conclusion

Locally, a high-efficiency design for crystal growth from melt using the Bridgman approach has been built and is being used to create $\text{Ti}_4\text{In}_3\text{GaS}_8$ crystals. The Hall coefficient and DC electrical conductivity were measured at temperatures ranging from 203 K to 443 K. The investigated samples possessed n-type conductivity with a R_H of $21.8 \text{ cm}^3\text{C}^{-1}$ at room temperature and carrier concentrations of $2.997 \times 10^{29} \text{ cm}^{-3}$. The energy gap E_g and the ionisation energy E_d were estimated to be 0.49 eV and 0.15 eV, respectively. The diffusion coefficient, diffusion length, and relaxation time were calculated for the majority of carries. The charge carrier scattering process was also examined. This investigation is necessary to provide a detailed overview of the synthesis and properties of this semiconductor compound. This can lead to more suitable applications in electronic devices.

References

- [1] Q. Guo, G. M. Ford, W. C. Yang, B. C. Walker, E. A. Stach, H. W. Hillhouse, R. Agrawal J. Am. Chem. Soc., 132 (2010), pp. 17384-17386 Finding PDF... CrossRefView Record in Scopus.
- [2] Tsuji, Y. Shimodaira, H. Kato, H. Kobayashi, A. Kudo Chem. Mater., 22 (2010), pp. 1402-1409 Finding PDF... CrossRefView Record in Scopus.
- [3] T. Fries, Y. Shapira, F. Palacio, M. C. Moron, G. J. McIntyre, R. Kershaw, A. Wold, E. J. McNiff Phys. Rev. B, 56 (1997), pp. 5424-5431 Finding PDF. View Record in Scopus.
- [4] G. Nenert, T. T. M. Palstra J. Phys. Condens. Matter, 21 (2009), p. 176002 6 pp. Finding PDF... CrossRefView Record in Scopus.
- [5] N. M. Gasanly, Journal of the Korean Physical Society, Vol. 50, No. 4, April 2007, pp. 1104-1108.

- [6] D. Muller and H. Hahn, Z. Anorg. Allg. Chemie 438, 258 (1978).
- [7] S. A. Hussein, and A. T. Nagat, Ctyst. Res. Technol. 24, 283 (1989).
- [8] I. ISENBERG, B. R. RUSSELL, and R. F GREENE, 1948, Rev. scient. Instrum., 19, 685-688.
- [9] S. R. Alharbi, Chin. Phys. B Vol. 22, No. 5 (2013) 058105.
- [10] J. A. M. Abdulwahed, January 2014Life Science Journal 11 (4): 109-113.
- [11] A. Salem, M. H. Alhossainy, Materials Chemistry and Physics Volume 263, 15 April 2021, 124436.
- [12] M. Guc, E. Lähderanta, +5 authors K. Lisunov Materials Science, Medicine Scientific Reports 2017.
- [13] Nagat, A. T., J. Phys. Condens. Matter, 1: 7921 (1989).